



ARL-TR-8202 • Nov 2017



Effect of Batch-to-Batch Variability on the Phase Transition of Precipitated Erbium-Doped Alumina Particles

by Nicholas Ku, Victoria L Blair, and Raymond E Brennan

Approved for public release; distribution is unlimited.

NOTICES

Disclaimers

The findings in this report are not to be construed as an official Department of the Army position unless so designated by other authorized documents.

Citation of manufacturer's or trade names does not constitute an official endorsement or approval of the use thereof.

Destroy this report when it is no longer needed. Do not return it to the originator.



Effect of Batch-to-Batch Variability on the Phase Transition of Precipitated Erbium-Doped Alumina Particles

by Nicholas Ku, Victoria L Blair, and Raymond E Brennan
Weapons and Materials Research Directorate, ARL

REPORT DOCUMENTATION PAGE

*Form Approved
OMB No. 0704-0188*

Public reporting burden for this collection of information is estimated to average 1 hour per response, including the time for reviewing instructions, searching existing data sources, gathering and maintaining the data needed, and completing and reviewing the collection information. Send comments regarding this burden estimate or any other aspect of this collection of information, including suggestions for reducing the burden, to Department of Defense, Washington Headquarters Services, Directorate for Information Operations and Reports (0704-0188), 1215 Jefferson Davis Highway, Suite 1204, Arlington, VA 22202-4302. Respondents should be aware that notwithstanding any other provision of law, no person shall be subject to any penalty for failing to comply with a collection of information if it does not display a currently valid OMB control number.

PLEASE DO NOT RETURN YOUR FORM TO THE ABOVE ADDRESS.

1. REPORT DATE (DD-MM-YYYY) November 2017		2. REPORT TYPE Technical Report		3. DATES COVERED (From - To) October 2015 – September 2017	
4. TITLE AND SUBTITLE Effect of Batch-to-Batch Variability on the Phase Transition of Precipitated Erbium-Doped Alumina Particles				5a. CONTRACT NUMBER	
				5b. GRANT NUMBER	
				5c. PROGRAM ELEMENT NUMBER	
6. AUTHOR(S) Nicholas Ku, Victoria L Blair, and Raymond E Brennan				5d. PROJECT NUMBER DSI14-WM014	
				5e. TASK NUMBER	
				5f. WORK UNIT NUMBER	
7. PERFORMING ORGANIZATION NAME(S) AND ADDRESS(ES) US Army Research Laboratory ATTN: RDRL-WMM-E Aberdeen Proving Ground, MD 21005				8. PERFORMING ORGANIZATION REPORT NUMBER ARL-TR-8202	
9. SPONSORING/MONITORING AGENCY NAME(S) AND ADDRESS(ES)				10. SPONSOR/MONITOR'S ACRONYM(S)	
				11. SPONSOR/MONITOR'S REPORT NUMBER(S)	
12. DISTRIBUTION/AVAILABILITY STATEMENT Approved for public release; distribution is unlimited.					
13. SUPPLEMENTARY NOTES					
14. ABSTRACT Alumina (Al ₂ O ₃ , aluminum oxide) is an excellent candidate as an optical material for laser gain media due to its high thermal conductivity. However, a rare earth (RE) cation dopant is necessary for the material to lase. To combat the dopant issue, nanosized alumina particles were synthesized via co-precipitation to trap RE ions in the alumina lattice before calcination. The wet co-precipitation process allowed for high purity and homogeneous distribution of the RE ions within the particles. A common issue with laboratory-scale synthesis is batch-to-batch variability. The reproducibility of the precipitated powder was investigated by holding the synthesis conditions constant. Variability of the phase transition temperature of alumina powder was tracked between batches, and showed a less than 1% difference in the transition temperature for gamma(γ)-alumina, as determined by high-temperature differential scanning calorimetry (HT-DSC).					
15. SUBJECT TERMS processing, alumina, synthesis, ceramics, nanoparticles, phase transition					
16. SECURITY CLASSIFICATION OF:			17. LIMITATION OF ABSTRACT UU	18. NUMBER OF PAGES 24	19a. NAME OF RESPONSIBLE PERSON Victoria Blair
a. REPORT Unclassified	b. ABSTRACT Unclassified	c. THIS PAGE Unclassified			19b. TELEPHONE NUMBER (Include area code) 410-306-4947

Contents

List of Figures	iv
Acknowledgments	v
1. Introduction	1
2. Method	2
2.1 Particle Synthesis	2
2.2 Measurements	5
3. Results and Discussion	5
4. Conclusions	11
5. References	12
List of Symbols, Abbreviations, and Acronyms	14
Distribution List	15

List of Figures

Fig. 1	Progression of various transition alumina phases and their crystal systems	2
Fig. 2	Schematic of the particle synthesis setup.....	4
Fig. 3	Differential scanning calorimetry of synthesized Er:Al ₂ O ₃ precursor powder.....	6
Fig. 4	X-ray diffraction pattern of synthesized Er:Al ₂ O ₃ precursor powder heat treated to 230 °C showing boehmite crystal structure PDF#98-000-0120	7
Fig. 5	X-ray diffraction pattern of synthesized Er:Al ₂ O ₃ precursor powder heat treated to 880 °C showing γ-alumina crystal structure PDF#98-000-0059	7
Fig. 6	X-ray diffraction pattern of synthesized Er:Al ₂ O ₃ precursor powder heat treated to 1350 °C showing α-alumina crystal structure PDF#98-000-0174	8
Fig. 7	Differential scanning calorimetry of 5 samples taken from the same batch of synthesized Er:Al ₂ O ₃ precursor powders.....	9
Fig. 8	Differential scanning calorimetry of 6 different batches of synthesized Er:Al ₂ O ₃ precursor powder using the same processing conditions	10
Fig. 9	Transition temperature of γ-alumina for 6 different batches of synthesized Er:Al ₂ O ₃ precursor powder measured from differential scanning calorimetry	10

Acknowledgments

This research was supported, in part, by an appointment to the Postgraduate Research Participation Program at the US Army Research Laboratory (ARL) administered by the Oak Ridge Institute for Science and Education through an interagency agreement between the US Department of Energy and ARL. The authors would also like to thank Dr Robert Pavlacka and Dr Tony Sutorik for their preliminary development of the synthesis method. The expertise and management of high-temperature furnace systems by Steven Kilczewski is also acknowledged.

INTENTIONALLY LEFT BLANK.

1. Introduction

Alumina, or aluminum oxide (Al_2O_3), is the most commonly used inorganic ceramic material. The α -phase of alumina, also known as corundum or sapphire (single crystal alumina), is the most common crystalline form, and is used in a variety of different applications, including electrical and thermal insulation, abrasives, wear-resistance materials, and structural ceramics.¹ Of specific interest to this work are the optical applications of alumina, as research has been focused on processing transparent materials with high thermal conductivities,^{2,3} making α -alumina a strong candidate as a gain material for high-energy laser (HEL) applications. High thermal conductivity allows for the laser material to be pumped far more aggressively with less thermally-induced optical distortion, and with minimal risk of mechanical failure due to buildup of thermal stresses. A common laser gain material currently being used, neodymium-doped yttrium aluminum garnet (Nd-YAG), has a thermal conductivity between 9 and 14 $\text{W m}^{-1} \text{K}^{-1}$, which is much lower than α -alumina. α -Alumina typically exhibits thermal conductivity between 30 to 35 $\text{W m}^{-1} \text{K}^{-1}$.³

Doping is required to make alumina lase, as most photoluminescent materials rely on rare earth (RE) dopants, which are more efficient and have lower lasing thresholds. Research has been conducted on RE-doped alumina materials ($\text{RE}:\text{Al}_2\text{O}_3$), with previous investigations concentrated on Tb^{3+4} and Eu^{3+} .⁵ For this study, erbium (Er^{3+}) was the RE dopant of interest. The wavelength emitted by an Er-doped laser gain material is 2940 nm, which matches the absorption of water, making it well-suited for laser surgery if the power requirement is met.⁶ Furthermore, Er-doped lasers emit in the spectral range of “eye-safe” laser radiation, as they do not penetrate the eye and cause permanent retina damage.⁷

A major challenge for doping RE ions into alumina, including Er^{3+} , is the ionic size mismatch between the dopant ions and the Al^{3+} cations that are replaced in the lattice.⁸ To facilitate homogeneous doping into the lattice, a wet-chemical precipitation method has been developed in which the cation species are mixed in-solution.⁹ Using this method, an alumina precursor powder was synthesized, incorporating a high-temperature calcination step to convert the precursor to α -alumina.^{10,11} The phase transition of alumina can follow many paths when starting with an aluminum hydroxide precursor. Generally, aluminum hydroxide powder starting with a boehmite structure follows a transition sequence of gamma, delta, theta, to alpha with increasing temperature, as shown in Fig. 1.¹²

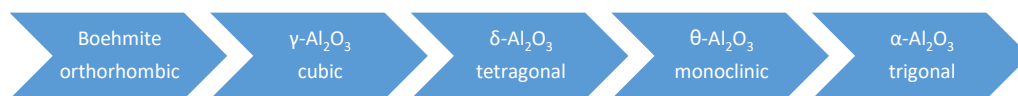


Fig. 1 Progression of various transition alumina phases and their crystal systems

While the work on alumina phase transitions is well established,¹² the addition of RE dopants is not well understood and can change the local structural properties of the alumina lattice due to the ionic size mismatch.¹³ Additionally, RE doping in alumina has been found to have a significant influence over its structural and phase evolution.⁸ The process of doping ions into the alumina lattice is a challenge. Previous studies on doped alumina ceramics used a dry mechanical method for doping ions,^{4,14} which led to the formation of dopant-rich regions at the grain boundaries. A wet chemical method for doping is expected to increase the homogeneity of the dopant within the lattice of the alumina.⁸

When synthesizing particles using a wet chemical process, slight variations in concentrations can affect the properties of the precipitated powders, such as particle size, phase, and crystallinity.^{15–17} These differences can affect the subsequent processing of the powders, such as the calcination temperature required to transform the powder to the desired phase, which for HEL applications is α -alumina due to its high mechanical strength and high thermal conductivity. For this study, a lab-scale synthesis process is used, which yields relatively small amounts of powder in 5-g targeted batches. When dealing with powder produced in small batches, the batch-to-batch variability in the powder properties can have a significant impact on the subsequent processing.

In this study, the phase evolution of precipitated alumina precursor powders doped with erbium using a wet chemical process will be investigated. The synthesized powder will be characterized using differential scanning calorimetry (DSC) and X-ray diffraction (XRD) to investigate the relevant phase transitions of the samples. To understand the reproducibility of this synthesis method, the shift in the phase transition temperatures between different batches will be measured.

2. Method

2.1 Particle Synthesis

Alumina powder with RE dopants were synthesized by a wet chemical synthesis process via precipitation in a technique similar to the one used by Sanamyan et al.⁹ The RE element investigated in these studies was Er. The starting materials were

all commercially available products from Alfa Aesar (Haverhill, MA), including aluminum nitrate nonahydrate (99.999%) ($\text{Al}[\text{NO}_3]_3 \cdot 9\text{H}_2\text{O}$), erbium nitrate pentahydrate (99.99%) ($\text{Er}[\text{NO}_3]_3 \cdot 5\text{H}_2\text{O}$), and magnesium nitrate hexahydrate (99.999%) ($\text{Mg}[\text{NO}_3]_3 \cdot 6\text{H}_2\text{O}$). All nitrates were tested by thermogravimetric analysis (TGA) to determine the exact amount of nitrate and chemical water for precise chemical composition of the synthesized powder. A solution was made in deionized (DI) H_2O with a nitrate concentration of 2.15 M. The composition of the cations in solution consisted of 400 ppm of Er^{3+} and 250 ppm of Mg^{2+} . Batches were calculated to yield 5 g of precursor powder.

The precipitation process for synthesizing alumina powder is shown in Fig. 2. A buffer solution of 0.25 M ammonium bicarbonate (NH_4HCO_3) was prepared, and the pH of this solution was adjusted to 7 using nitric acid (HNO_3). The acidic nitrate solution, along with a basic solution, which consisted of 65 g ammonium hydroxide (NH_4OH) and 235 g NH_4HCO_3 in 2000 g DI H_2O , was simultaneously added to the buffer drop by drop. As the 2 solutions were mixed into the buffer solution, the doped alumina precursor particles began to precipitate out into suspension. The drip rate of the acidic nitrate solution was kept constant using a Control Company Model 3386 flow pump (Friendswood, TX). The drip rate of the basic solution was adjusted using a buret to maintain the pH of the bath at 7 for the duration of the synthesis process. The pH of the suspension was continuously monitored during the precipitation process by an Oakton pH 2500 probe (Vernon Hills, IL). During the entire titration process, the suspension was continuously mixed using a magnetic stir bar.

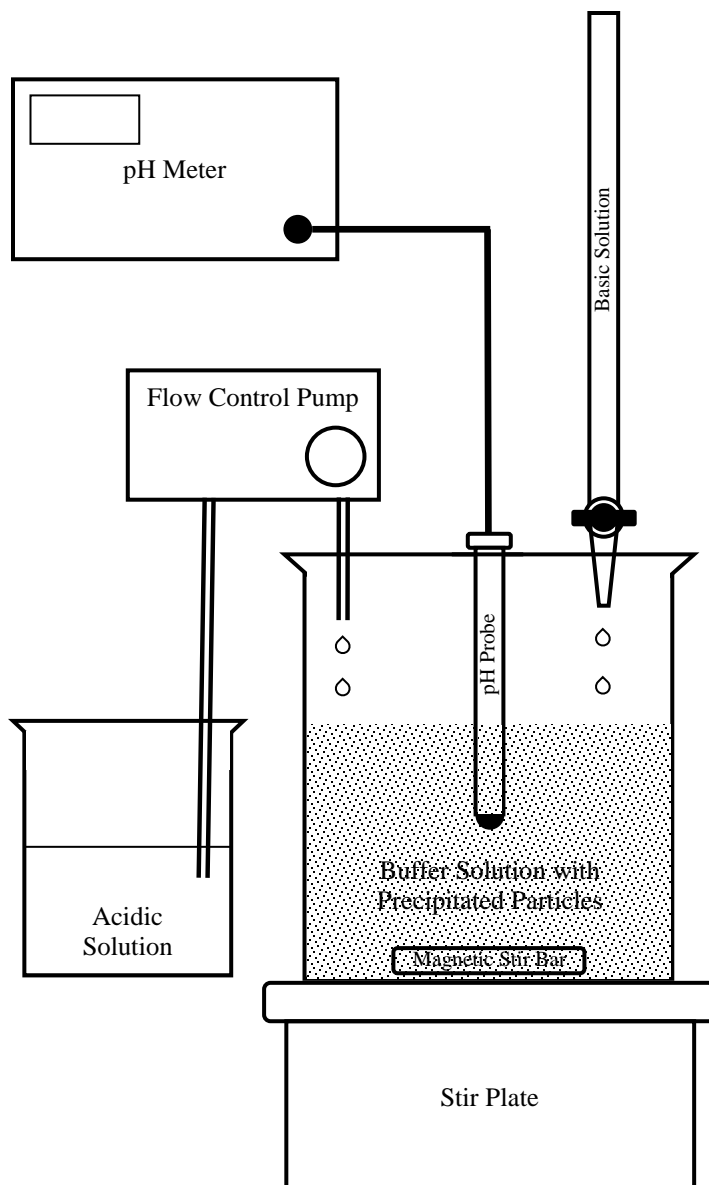


Fig. 2 Schematic of the particle synthesis setup

After the precipitation process was completed, the suspension was stirred overnight to allow the reaction to complete before being filtered through nitrocellulose membranes with 0.22 μm openings. The particles were collected and dispersed in DI H_2O and filtered twice to wash off any remnant salts that resulted from synthesis. Finally, the particles were dispersed in isopropanol to aid in drying, and filtered before being placed in an oven at 70 $^\circ\text{C}$. Once dried, the precursor powder was gently crushed using a silica glass mortar and pestle.

2.2 Measurements

Calorimetry was measured using a TA Instruments SDT Q600 DSC-TGA (New Castle, DE). Precursor powder samples were evaluated up to 1400 °C at a heating rate of 10 °C/min under flowing argon (Ar). Calcination of powder was conducted in a CM Furnaces (Bloomfield, NJ) Model 1710 FL. The heating rate was 10 °C/min ramp up and down from the target temperature, using a dwell time of 30 min for all samples. The phases of the ground powder were identified by XRD, using a Rigaku MiniFlex II X-ray diffractometer (Tokyo, Japan). The diffraction patterns were analyzed using commercially available Jade (MDI Inc.) software.

3. Results and Discussion

Fig. 3 shows the DSC data for a batch of Er:Al₂O₃. A positive heat flow denotes an exothermic reaction, while a negative heat flow indicates an endothermic reaction. From the synthesis process, the powder was amorphous, with a chemical composition of ammonium aluminum carbonate hydroxide. Upon heating, the powder decomposed, showing an endothermic heat flow, which had a local peak at approximately 200 °C. Subsequent phase transitions occurred as the crystalline phase of the material evolved. The most noticeable phase transitions, as marked by local exothermic peaks, were seen at roughly 870 °C and 1300 °C. To probe the powder phases, 3 samples of powder were collected from the same batch and calcined to temperatures just over the transition temps measured by DSC. The phases of the calcined powders were then identified using XRD.

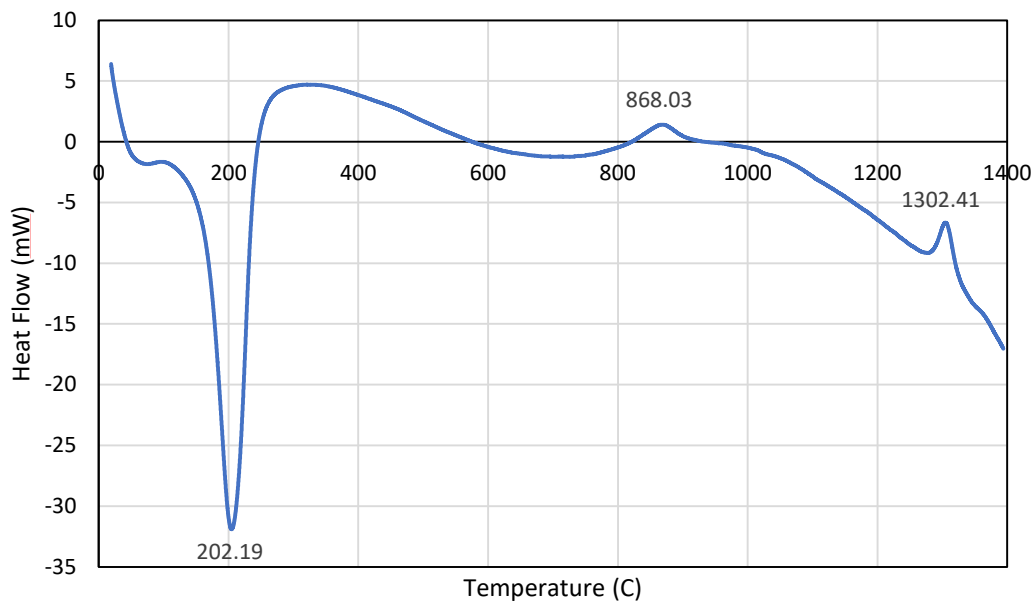


Fig. 3 Differential scanning calorimetry of synthesized Er:Al₂O₃ precursor powder

Fig. 4 through 6 show the phases of the powder probed around the 3 previously mentioned temperatures. For each sample, powder was calcined to a temperature just above the peaks measured on the DSC in Fig. 3. In Fig. 4, the precursor powder was heated to 230 °C, and the resultant diffraction pattern was indicative of boehmite. The boehmite exhibited broad peaks in the diffraction pattern, which was expected in the nanosized powder. Fig. 5 shows the diffraction pattern of the powder after being heated to 880 °C. The phase had transitioned to γ -alumina, although the peaks remained broad due to the fine sizes of the crystallites. At 1350 °C, the diffraction pattern of the powder is shown in Fig. 6, with the phase being that of α -alumina. Due to the increased temperature that was reached, the crystallites had coarsened, which was indicated by the more narrow peaks in the diffraction pattern. No secondary Er-rich phase was detected in any of the phases. Having the dopants migrate out of the lattice and form secondary phases is undesirable for HEL applications due to reducing transmission through the material by creating scattering points.

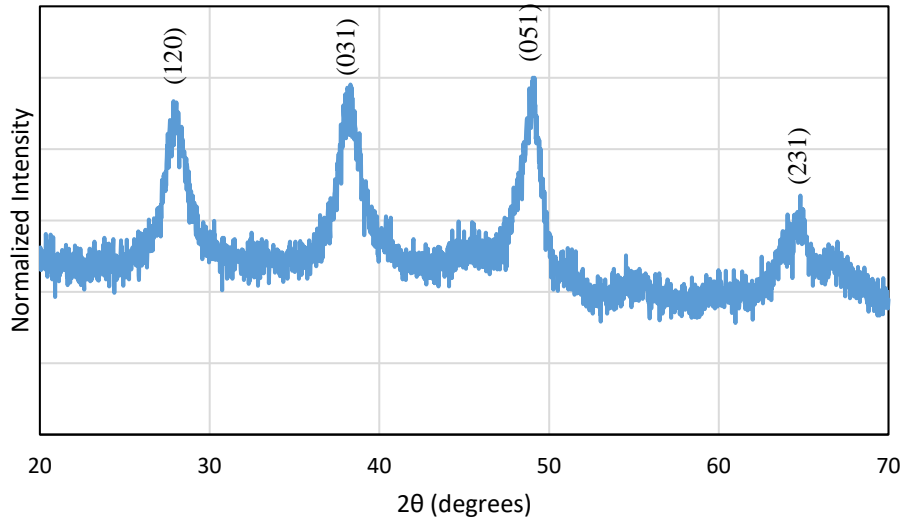


Fig. 4 X-ray diffraction pattern of synthesized Er:Al₂O₃ precursor powder heat treated to 230 °C showing boehmite crystal structure PDF#98-000-0120

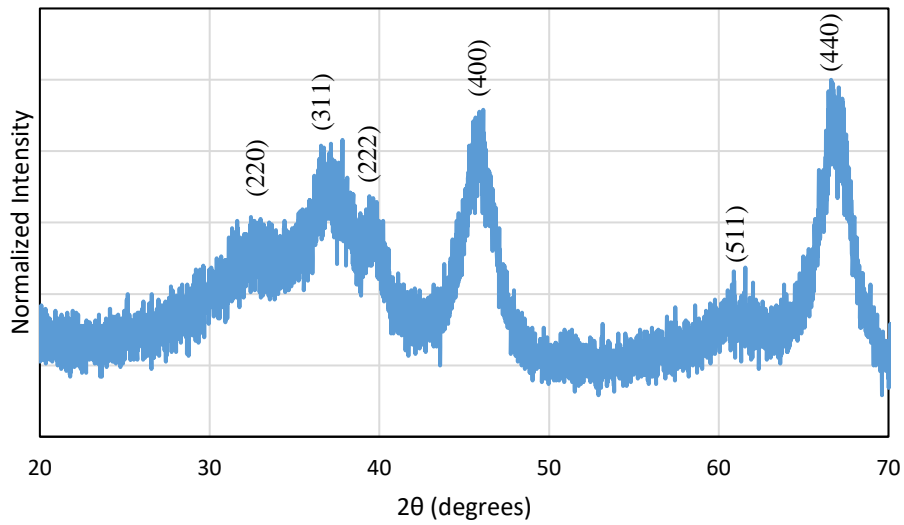


Fig. 5 X-ray diffraction pattern of synthesized Er:Al₂O₃ precursor powder heat treated to 880 °C showing γ-alumina crystal structure PDF#98-000-0059

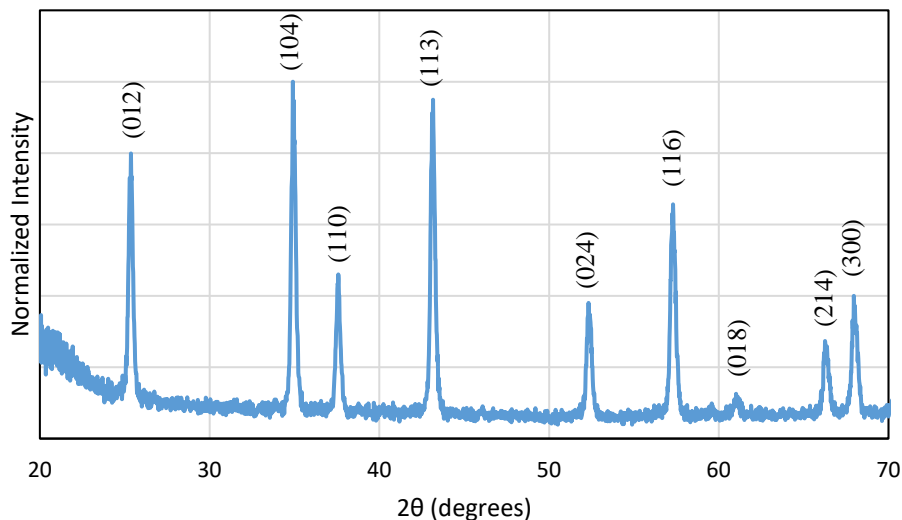


Fig. 6 X-ray diffraction pattern of synthesized Er:Al₂O₃ precursor powder heat treated to 1350 °C showing α -alumina crystal structure PDF#98-000-0174

To understand the reproducibility of the DSC measurement, a batch of precursor powders was synthesized and 5 separate samples from the batch were collected. Each sample was measured in the DSC. The heat flow data for each of the samples as a function of increasing temperature is shown in Fig. 7. For each sample, the temperature of the exothermic peak related to the γ -alumina phase transition was measured. The peak location varied from 866.04 °C to 868.95 °C in the 5 samples, with an average temperature of 867.43 °C and a standard deviation of 1.13 °C. The low standard deviation indicated a high confidence in the measurement.

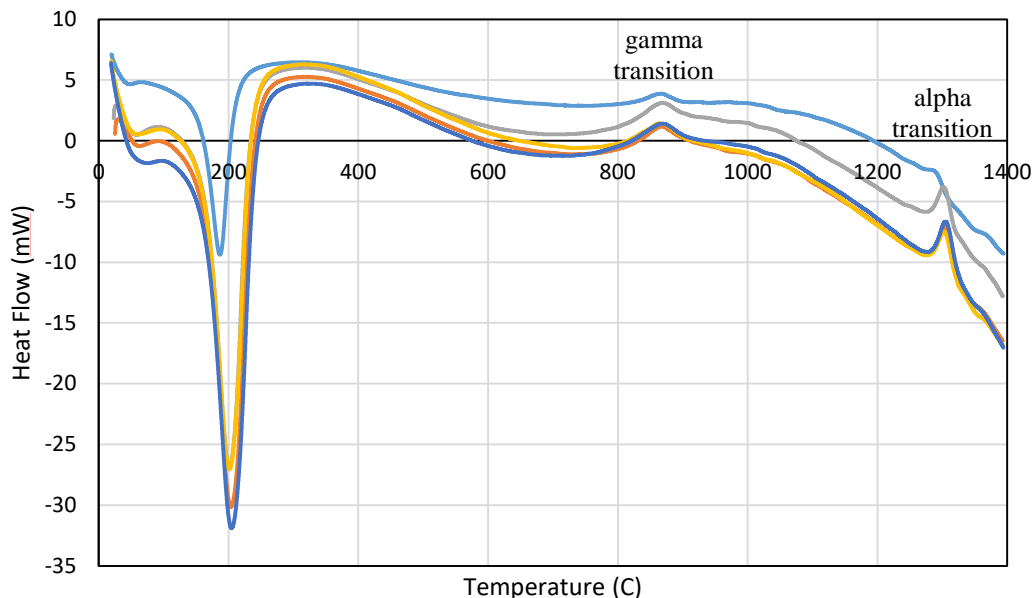


Fig. 7 Differential scanning calorimetry of 5 samples taken from the same batch of synthesized Er:Al₂O₃ precursor powders

Six separate batches of precursor powder of the same composition were synthesized using the same processing conditions. The 6 batches were each measured using the DSC to observe any variability from batch to batch, as shown in Fig. 8. The temperature of the exothermic peak related to the γ -alumina phase transition was used as the indicator for each batch. The transition temperature for each batch is shown in Fig. 9. The error bars in the graph refer to the standard deviation of the DSC measurements, which were discussed in the previous paragraph. The temperatures ranged from 867.43 °C to 873.42 °C. Of the 6 batches measured, only Batch #1 was an outlier, with Batches #2–6 all within the error of the measurement. Given the precision of the DSC measurement, the difference in the γ -alumina phase transition temperature from batch to batch was significant enough to be measured by the instrument. Nevertheless, the range in the data indicated a difference of less than 1%, and did not appear to be significant, given the general processing conditions.

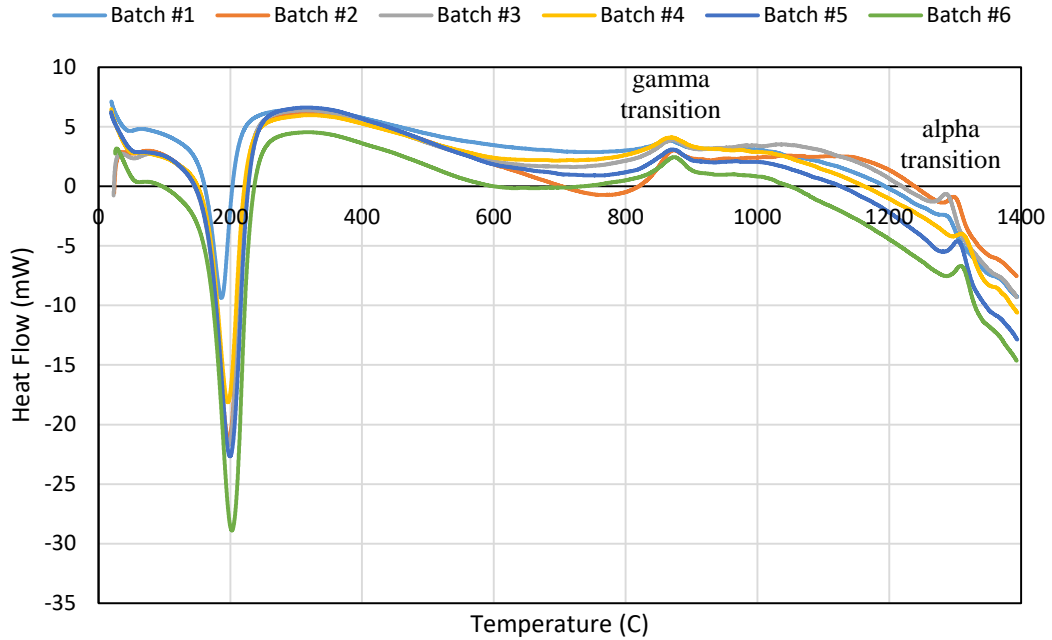


Fig. 8 Differential scanning calorimetry of 6 different batches of synthesized Er:Al₂O₃ precursor powder using the same processing conditions

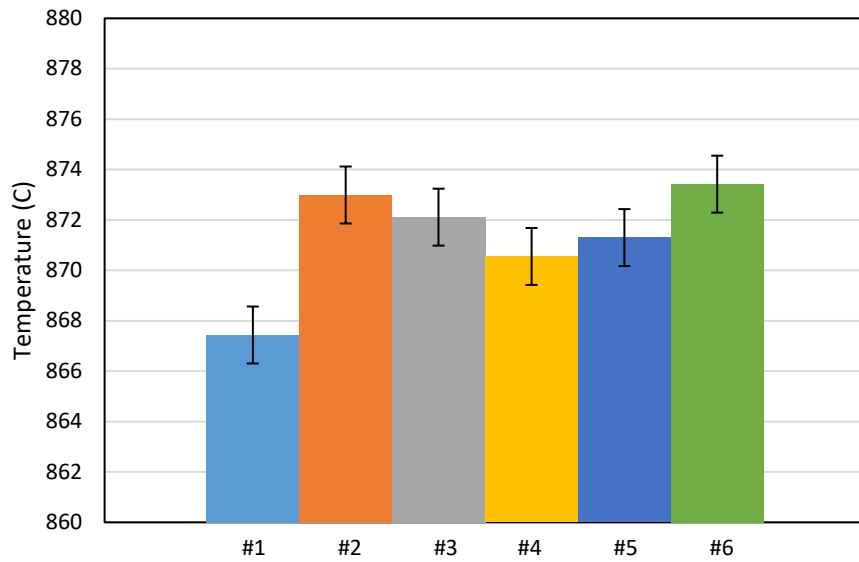


Fig. 9 Transition temperature of γ -alumina for 6 different batches of synthesized Er:Al₂O₃ precursor powder measured from differential scanning calorimetry

The variations in transition temperature from batch to batch could likely be explained by the slight physical variations in the powder. While synthesis conditions such as the pH of the nitrate solution and the rate of mixing were controlled, temperature and relative humidity of the laboratory were not.

Additionally, the temperature of the buffer solution during precipitation was not controlled. While the process was conducted at room temperature, any change in temperature in the suspension during the precipitation was not monitored. These factors may have led to differences in crystallite size,¹⁵ indicating that the variability in the batches was due to differences in starting particle size. Furthermore, the addition of the RE dopants in the alumina lattice had already shown an effect on the phase transition temperatures⁸ and the results may illustrate a more pronounced effect on the synthesized alumina as the sensitivity of those transitions with the Er dopant has not been investigated.

This research demonstrated the robustness of using a wet chemical process to synthesize erbium-doped alumina powder. Additional work needs to be conducted on the stability of the erbium dopant within the alumina lattice. The current heating regime uses a relatively short dwell time of 30 min at a maximum temperature of 1350 °C. If the material is subjected to higher temperatures and longer dwell times, which may be necessary to sinter this powder into a dense ceramic, the erbium dopant may have the energy and time to diffuse out of the lattice and form a secondary erbium-rich phase. This is undesirable for optical applications, as secondary phases act as scattering points that reduce transmission. For this reason, future work should be concentrated on the stability of the dopant within the lattice at elevated temperatures.

4. Conclusions

Er:Al₂O₃ powder was synthesized using a wet chemical precipitation process. The phase transition temperatures of the precursor powder were tracked using DSC and confirmed by XRD. At 230 °C, 880 °C, and 1350 °C, the phases of the powder were boehmite, γ -alumina, and α -alumina, respectively. The variability from batch to batch of the synthesized powder was determined by measuring the γ -alumina transition temperature, which was less than 1%, although significant enough to be measured by the DSC. While this variation was minimal, it must be taken into account when calcining batches of precipitated alumina precursor powder synthesized using this method.

5. References

1. Reed JS. Principles of ceramics processing. 2nd ed. New York (NY): John Wiley & Sons, Inc. 1995.
2. Coble RL. Transparent alumina and method of preparation. Google Patents US 3026210 A. 1962.
3. Barsoum M, Barsoum MW. Fundamentals of ceramics. CRC Press; 2002.
4. Penilla EH, Kodera Y, Garay JE. Blue–green emission in terbium-doped alumina (Tb:Al₂O₃) transparent ceramics. *Adv Funct Mater.* 2013;23(48):6036–6043.
5. Reis DH, Buarque JM, Schiavon MA, Pecoraro E, Ribeiro SJL, Ferrari JL. Simple and cost-effective method to obtain RE³⁺-doped Al₂O₃ for possible photonic applications. *Ceram Int.* 2015;41(9):10406–10414.
6. Bader C, Krejci I. Indications and limitations of Er:YAG laser applications in dentistry. *Am J Dent.* 2006;19(3):178–86.
7. Mierczyk Z, Kwaśny M, Kopczyński K, Gietka A, Łukasiewicz T, Frukacz Z, Kisielewski J, Stępień R, Jędrzejewski K. Er³⁺ and Yb³⁺ doped active media for ‘eye safe’ laser systems. *J Alloy Compd.* 2000;300:398–406.
8. Patel K, Blair V, Douglas J, Dai Q, Liu Y, Ren S, Brennan R. Structural effects of lanthanide dopants on alumina. *Sci Rep.* 2017;7:39946.
9. Sanamyan T, Pavlacka R, Gilde G, Dubinskii M. Spectroscopic properties of Er³⁺-doped α-Al₂O₃. *Opt Mater.* 2013;35(5):821–826.
10. Zhang HJ, Xiu EX, Wang XJ, Jia QL, Sun HW, Jia XL. Thermal decomposition kinetics of ammonium aluminum carbonate hydroxide. *Key Eng Mater. Trans Tech Publ.* 2008:1577–1579.
11. Parida K, Pradhan AC, Das J, Sahu N. Synthesis and characterization of nano-sized porous gamma-alumina by control precipitation method. *Mater Chem Phys.* 2009;113(1):244–248.
12. Wefers K, Misra C. Oxides and hydroxides of aluminum [Alcoa technical paper no. 19, revised]. Pittsburgh (PA): Aluminum Company of America (US); Alcoa Laboratories; 1987.
13. Limmer KR, Neupane MR, Brennan RE, Chantawansri TL. Rare-earth dopant effects on the structural, energetic, and magnetic properties of alumina from first principles. *J Am Ceram Soc.* 2016;99(12):4007–4012.

14. Penilla EH, Hardin CL, Kodera Y, Basun SA, Evans DR, Garay JE. The role of scattering and absorption on the optical properties of birefringent polycrystalline ceramics: modeling and experiments on ruby (Cr:Al₂O₃). *J Appl Phys.* 2016;119(2):023106.
15. Okada K, Nagashima T, Kameshima Y, Yasumori A, Tsukada T. Relationship between formation conditions, properties, and crystallite size of boehmite. *J Colloid Interface Sci.* 2002;253(2):308–314.
16. Jolivet J-P, Cassaignon S, Chanéac C, Chiche D, Durupthy O, Portehault D. Design of metal oxide nanoparticles: control of size, shape, crystalline structure and functionalization by aqueous chemistry. *CR Chim.* 2010;13(1):40–51.
17. Jolivet J-P, Chanéac C, Chiche D, Cassaignon S, Durupthy O, Hernandez J. Basic concepts of the crystallization from aqueous solutions: the example of aluminum oxy(hydroxi)des and aluminosilicates. *CR Geosci.* 2011;343(2):113–122.

List of Symbols, Abbreviations, and Acronyms

Ar	argon
ARL	US Army Research Laboratory
DI	deionized
DSC	differential scanning calorimetry
Er	erbium
HEL	high-energy laser
HT-DSC	high-temperature differential scanning calorimetry
Nd-YAG	neodymium-doped yttrium aluminum garnet
RE	rare earth
TGA	thermogravimetric analysis
XRD	X-ray diffraction

1 DEFENSE TECHNICAL
(PDF) INFORMATION CTR
DTIC OCA

2 DIR ARL
(PDF) IMAL HRA
RECORDS MGMT
RDRL DCL
TECH LIB

1 GOVT PRINTG OFC
(PDF) A MALHOTRA

3 DIR ARL
(PDF) RDRL WM
J ZABINSKI
RDRL WMM
M VANLANDINGHAM
RDRL WMM E
N KU
V BLAIR
R BRENNAN
S SILTON
L VARGAS

INTENTIONALLY LEFT BLANK.